International Journal of Mechanical Systems Engineering
Research Article Open Access

Dynamic Behavior of Functionally Graded Beams in Thermal Environment due to a Moving Harmonic Load

Thanh Huong Trinh[1], Van Tuyen Bui[2], Ngoc Huyen Nguyen[2], DinhKien Nguyen[3] and Buntara S. Gan[1*]

[1]*Department of Architecture, College of Engineering, Nihon University, Japan*
[2]*Thuy Loi University, 175 Tay Son, Dong Da, Hanoi, Vietnam*
[3]*Institute of Mechanics, VAST, 18 Hoang Quoc Viet, Hanoi, Vietnam*

Abstract

This paper investigates the dynamic behavior of functionally graded beam in the thermal environment due to a moving harmonic load. The material properties are assumed to be graded in the thickness direction by a power-law function, and they are considered to be temperature dependent. Two types of temperature distribution, namely uniform and nonlinear temperature rises, are considered. Equations of motion based on Euler-Bernoulli beam theoryare derived from Hamilton's principle and they are solved by a simple finite element formulation in combination with Newmark time-integration procedure. Numerical results show that the dynamic deflection and dynamic amplification factor is decreased with increasing the temperature rise, and the decreasein the uniform temperature rise is more significant that by the nonlinear temperature rise. The excitation frequency plays an important role in the dynamic behavior of the beams, and the frequency at which resonant phenomenon can occur depends on the temperature. A parametric study is carried out to highlight the effect of the temperature rise and moving load parameters on the dynamic behavior of the beams.

Publication History:
Received: July 04, 2016
Accepted: October 03, 2016
Published: October 05, 2016

Keywords:

Functionally graded beam, Thermal environment, Temperature dependent material property, Moving harmonic load, Dynamic analysis

Introduction

Functionally graded materials (FGMs) were firstly developed by a Japanese scientist in mid-1980s as structural components for using in severe thermal conditions [1]. The smooth variation of the effective material properties enables these materials to overcome the drawbacks of the conventional composite materials. Many investigations on the behaviour of FGM structures in the thermal environment have been reportedin the literature, contributions that are most relevant to the present work are briefly discussed below.

Employing the Rayleigh-Ritz method, Kim [2] studied the free vibration of a third-order shear deformable FGM plate in the thermal environment. The author has shown that the frequency of the plate is remarkably decreased by the temperature rise. Pradhan and Murmu [3] used the modified differential quadrature method in solving the equations of motion for free vibration of elastically foundation supported FGM sandwich beams in a high-temperature environment. Based on the higher-order shear deformation theory, Mahi et al. [4] derived an analytical solution for free vibration of FGM beams with temperature-dependent material properties. The improved third-order shear deformation theory was used by Wattanasakulpong et al. [5] to study the thermal buckling and free vibration of FGM beams. The authors concluded that the fundamental frequency of the beams approaches zero when the temperature raises towards the critical temperature. Ebrahimi et al. [6] employed the differential quadrature method to study the free vibration of FGM porous beams in the thermal environment. It has been shown by the authors that the fundamental frequency of the beams is significantly influenced by both the temperature and porosities.

The vibration of beams due to moving loads is often met in practice and isa subject of investigation for a long time. A large number of closed-form solutions for homogeneous beams subjected to different types of moving loads are presented in a well-known monograph by Frýba [7]. The dynamic analysis of FGM beams due to moving loads has been carried out by several researchers recently. Şimşek and Kocatürk [8] approximated the axial and transverse displacements by polynomials in their derivation of the equations of motion for an FGM Euler-Bernoulli beam under a moving harmonic load. Lagrange multiplier method was then employed in combination with Newmark method to compute the vibration characteristics of the beams. The method in [8] has been extended by Şimşek in studying the dynamic behavior of FGM beams under a moving mass [9], and a nonlinear FGM Timoshenko beam subjected to a moving harmonic load [10]. Khalili et al. [11] used the mix Ritz-differential quadrature method to compute the dynamic response of FGM Euler-Bernoulli beams carrying moving loads. The Runge-Kutta method was employed by Rajabi et al. [12] to investigate the dynamic behavior of an FGM Euler-Bernoulli beam under a moving oscillator. Nguyen et al. [13], Gan et al. [14] employed the finite element method to study the dynamic behavior of FGM beams traversed by moving forces.

To the authors' best knowledge, the dynamic behavior of FGM beams in the thermal environment due to a moving harmonic load has not been studied in the literature, and it will beconsidered in the present work. The material properties are considered to be dependent on the temperature, and they are graded in the thickness direction by a power-law distribution. The temperature is assumed to vary in the beam thickness only, and its distribution is obtained from the steady-state Fourier equation. Theequations of motion based onEuler-Bernoulli beam theory are derived from Hamilton's principle and they are solved by a finite element formulation in combination with the Newmark time-integration method. The effect of the material distribution, temperature change, and moving load parameters on the on the dynamic behavior of the beams is examined in detail and highlighted.

***Corresponding Author:** Prof. Buntara Sthenly Gan, Department of Architecture, College of Engineering, Nihon University, Kanda Surugadai, 1−8−14, Tokyo 01-8308, Japan; E-mail: buntara@arch.ce.nihon-u.ac.jp

Citation: Trinh TH, Bui VT, Nguyen NH, Nguyen D, Gan BS (2016) Dynamic Behavior of Functionally Graded Beams in Thermal Environment due to a Moving Harmonic Load. Int J Mech Syst Eng 2: 119 . http://dx.doi.org/10.15344/2455-7412/2016/119

Functionally Graded Beam

A simply supported FGM beam with rectangular cross section under a load $F=F_0\cos(\Omega t)$, moving from right to left, as shown in Figure 1is considered. Denoting the length, cross-sectional height and width of the beam as *L, h* and *b*, respectively. The x-axis is chosen to be on the mid-plane, and the z-axis is perpendicular to the mid-plane. The investigation is carried out based on thefollowing assumptions: (i) the load *F* is always in contact with the beam, and its velocity (*v*) is constant; (ii) the beam is initially at rest, and the inertial effect of the load *F* is negligible.

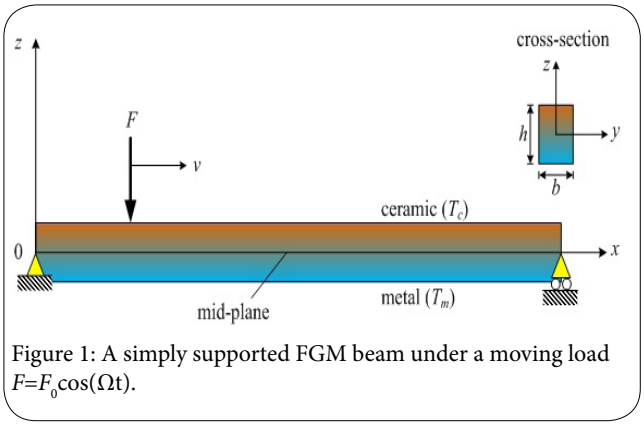

Figure 1: A simply supported FGM beam under a moving load $F=F_0\cos(\Omega t)$.

The beam material is formed fromceramic and metal with volume fraction of ceramic (V_c) and metal (V_m) is assumed to be given by

$$V_c = \left(\frac{z}{h}+\frac{1}{2}\right)^n \quad , \quad V_m + V_c = 1 \tag{1}$$

where n ($0 \le n < \infty$) is the grading index. In (1) and hereafter, the subscript "*c*" and "*m*" are used to indicate ceramic and metal, respectively.

The beam material is considered to be dependent on the temperature, and a typical property (P) is a function of temperature (T) as [15]

$$P = P_0\left(P_{-1}T^{-1} + 1 + P_1T + P_2T^2 + P_3T^3\right) \tag{2}$$

where $T=T_0+\Delta T$, with T_0 = 300 K is reference temperature and ΔT is the temperature rise, is the current environment temperature; P_{-1}, P_0, P_1, P_2 and P_3 are coefficients of T and they are unique to the constituents. Table 1 lists the coefficients of Alumina (Al_2O_3) and Steel (SUS304), the constituents of the beam considered in this paper.

The effective material properties are evaluated by Voigt's model read

$$P(z,T) = P_c(T)V_c + P_m(T)V_m \tag{3}$$

From Eqs. (1) and (3), the effective Young's modulus, thermal expansion and mass density are given by

$$\begin{aligned} E(z,T) &= [E_c(T) - E_m(T)]\left(\frac{z}{h}+\frac{1}{2}\right)^n + E_m(T) \\ \alpha(z,T) &= [\alpha_c(T) - \alpha_m(T)]\left(\frac{z}{h}+\frac{1}{2}\right)^n + \alpha_m(T) \\ \rho(z) &= (\rho_c - \rho_m)\left(\frac{z}{h}+\frac{1}{2}\right)^n + \rho_m \end{aligned} \tag{4}$$

where the mass density is considered to be independent of the temperature.

In the present work, the temperature is considered to vary in the thickness direction only, and itis assumed that the temperature being imposed to T_m at the bottom surface and T_c at the top surface. With this condition, the distribution of temperature in the thickness can be obtained as solution of the following Fourier equation (23)

$$-\frac{d}{dz}\left[\kappa(z)\frac{dT}{dz}\right] = 0 \tag{5}$$

where κ is the thermal conductivity, assumed to be independentof the temperature. The solution of Eq. (5) has the form (23)

$$T = T_c + \frac{(T_c - T_m)}{\int_{-h/2}^{h/2}\frac{1}{\kappa(z,T)}dz}\int_{-h/2}^{z}\frac{1}{\kappa(z,T)}dz \tag{6}$$

If $T_c = T_m$, Eq. (6)gives a uniform temperature rise(UTR). Otherwise, it describes a nonlinear temperature rise (NLTR).

Governing equation

Based on the Euler-Bernoulli beam theory, the displacements u and w of an arbitrary point in the x and z directions, respectively are given by

$$\begin{aligned} u(x,z,t) &= u_0(x,t) - zw_{0,x} \\ w(x,z,t) &= w_0(x,t) \end{aligned} \tag{7}$$

where u_0(x, t) and w_0(x, t) are respectively the axial and transverse displacements of a point on the *x*-axis; *t* is the time, and (...), *x* denotes the derivative with respect to *x*. Based on linearly elastic behaviour, the normal strain (ε_x) and normal stress (σ_x) are as follows

$$\varepsilon_x = u_{0,x} - zw_{0,xx}, \sigma_x = E(z,T)\varepsilon_x = E(z,T)(u_{0,x} - zw_{0,xx}) \tag{8}$$

The strain energy of the beam (U_B) resulted from the mechanical loads reads

Material	Property	P_0	P_{-1}	P_1	P_2	P_3
Al_2O_3	E (Pa)	349.55e+9	0	-3.853e-4	4.027e-7	-1.673e-10
	ρ (kg/ m³)	3800	0	0	0	0
	α (K-1)	6.8269e-6	0	1.838e-4	0	0
	κ(Wm/K)	-14.087	-1123.6	-6.227e-3	0	0
SUS304	E (Pa)	201.04e+9	0	3.079e-4	-6.534e-7	0
	ρ(kg/ m³)	8166	0	0	0	0
	α (K^{-1})	12.330e-6	0	8.085e-4	0	0
	κ(Wm/K)	15.379	0	-1.264e-3	2.092e-6	-7.223e-10

Table 1. Temperature-dependent coefficients of Young's modulus *E*, mass density *ρ*, coefficient of thermal expansion α and thermal conductivity *κ* for Al_2O_3 and SUS304 (32).

$$U_B = \frac{1}{2}\int_0^L\int_A \sigma_x \varepsilon_x dA dx \tag{9}$$

$$= \frac{1}{2}\int_0^L \left[A_{11} u_{0,x}^2 - 2A_{12} u_{0,x} w_{0,xx} + A_{22} w_{0,xx}^2 \right] dx$$

where A_{11}, A_{12} and A_{22} are respectively the extensional, extensional-bending coupling and bending rigidities, defined as

$$(A_{11}, A_{12}, A_{22}) = \int_A E(z,T)\left(1, z, z^2\right) dA \tag{10}$$

With A is the cross-sectional area. With the effective Young's modulus and temperature are given by Eqs. (4) and (6), the above rigidities can be evaluated.

The strain energy from initial stress due to the temperature rise (U_T) is given by [4]

$$U_T = \frac{1}{2}\int_0^L N_T \mathrm{w}_{0,x}^2 dx \tag{11}$$

where N_T is the axial force resultant caused by elevated temperature, defined as

$$N_T = -\int_A E(z,T)\alpha(z,T)\Delta T dA \tag{12}$$

with ΔT, as mentioned above, is the temperature rise. The kinetic energy of the beam (T) resulted from Eq. (7) is

$$\mathrm{T} = \frac{1}{2}\int_0^L\int_A \rho(z)(\dot{u}^2 + \dot{w}^2) dA dx \tag{13}$$

$$= \frac{1}{2}\int_0^L \left[I_{11}\left(\dot{u}_0^2 + \dot{w}_0^2\right) - I_{12}\dot{u}_0\dot{w}_{0,x} + I_{22}\dot{w}_{0,x}^2 \right] dx$$

where an overdot denotes the differentiation with respect to time, and I_{11}, I_{12}, I_{22} are the mass moments defined as

$$\left(I_{11}, I_{12}, I_{22}\right) = \int_A \rho(z)\left(1, z, z^2\right) dA \tag{14}$$

Finally, the potential of the moving forces (V) has a simple form as

$$V = -F_0 \cos(\Omega t) w_0(x,t)\delta\left(x - vt\right) \tag{15}$$

with $\delta(.)$ is the delta Dirac function; x is the current position of load F with respect to the left end of the beam.

Applying Hamilton's principle to Eqs. (9), (11), (13) and (15), we obtain the following equations of motion for the beam

$$I_{11}\ddot{u}_0 - I_{12}\ddot{w}_{0,x} - A_{11}u_{0,xx} + A_{12}w_{0,xxx} = 0 \tag{16}$$

$$I_{11}\ddot{w}_0 + I_{12}\ddot{u}_{0,x} - I_{22}\ddot{w}_{0,xx} - A_{12}u_{0,xxx} + A_{22}w_{0,xxxx} - N_T w_{0,xx}$$

$$= F_0 \cos(\Omega t)\delta(x - vt)$$

The natural boundary conditions for the beam are as follows

$$A_{11}u_{0,x} - A_{12}w_{0,xx} = \bar{N} \quad \text{at } x = 0 \text{ and } x = L \text{ or } u_0(0,t) = 0 \tag{17}$$

$$-A_{12}u_{0,xx} + A_{22}w_{0,xxx} = \bar{Q} \quad \text{at } x = 0 \text{ and } x = L \text{ or } \mathrm{w}_0(0,t) = \mathrm{w}_0(L,t) = 0$$

$$A_{12}u_{0,x} - A_{22}w_{0,xx} = \bar{M} \text{ at } x = 0 \text{ and } x = L$$

where are respectively the prescribed axial, shear forces and moments at the beam ends.

The finite element method is employed herein for solving Eq. (16). To this end, the beam is assumed to be divided into some two-node elements with a length of l. The vector of nodal displacements (d) for a generic element has six components as

$$\mathbf{d} = \left\{ u_1 \;\; w_1 \;\; \theta_1 \;\; u_2 \;\; w_2 \;\; \theta_2 \right\}^T \tag{18}$$

where u_1, u_2 are respectively the axial displacements at nodes 1 and 2; w_1, θ_1, w_2, θ_2 are the transverse displacements and rotations at the two nodes. In Eq. (18) and hereafter the superscript 'T' is used to denote a transpose of a vector or a matrix.

The axial displacement u and transverse displacement ware interpolated from the nodal values according to

$$u_0 = \mathbf{H}_u\mathbf{u}\,,\; w_0 = \mathbf{H}_w\mathbf{w} \tag{19}$$

where $\mathbf{H}_u = \{H_{u1}\,0\,0\,H_{u2}\,0\,0\}$, $\mathbf{H}w = \{0\;H_{w1}H_{w2}\,0\;H_{w3}H_{w4}\}$ are the matrices of shape functions. Here, the following linear and cubic Hermite polynomials are used as the shape functions for u and w

$$H_{u1} = \frac{l - x}{l}, \quad H_{u2} = \frac{x}{l} \tag{20}$$

and

$$H_{w1} = 1 - 3\frac{x^2}{l^2} + 2\frac{x^3}{l^3}, \quad H_{w2} = x - 2\frac{x^2}{l} + \frac{x^3}{l^2}$$

$$H_{w3} = 3\frac{x^2}{l^2} - 2\frac{x^3}{l^3}, \quad H_{w4} = -\frac{x^2}{l} + \frac{x^3}{l^2} \tag{21}$$

Using the above shape functions, one can write the strain energy U_B in the form

$$U_B = \frac{1}{2}\sum_{i=1}^{ne} \mathbf{d}_i^T \mathbf{k}_{Bi} \mathbf{d}_i \tag{22}$$

where $\mathbf{k}_T$ is the element stiffness matrix due to the mechanical load with the following form

$$\mathbf{k}_B = \int_0^l (\mathbf{H}_{u,x}^T A_{11} \mathbf{H}_{u,x} - \mathbf{H}_{u,x}^T A_{12} \mathbf{H}_{w,xx} + \mathbf{H}_{w,xx}^T A_{22} \mathbf{H}_{w,xx}) dx \tag{23}$$

The strain energy resulted from the temperature rise can be written as

$$U_T = \frac{1}{2}\sum_{i=1}^{ne} \mathbf{d}_i^T \mathbf{k}_{Ti} \mathbf{d}_i \tag{24}$$

where $\mathbf{k}_T$ is the stiffness matrix stemming from the temperature rise with the following form

$$\mathbf{k}_T = \int_0^l \mathbf{H}_{w,x}^T N_T \mathbf{H}_{w,x} dx \tag{25}$$

Similarly, the kinetic energy can be written as

$$\mathrm{T} = \frac{1}{2}\sum_{i=1}^{ne} \dot{\mathbf{d}}_i^T \mathbf{m}_i \dot{\mathbf{d}}_i \tag{26}$$

with the element consistent mass matrix m has the form

$$\mathbf{m} = \int_0^l \left(\mathbf{H}_u^T I_{11} \mathbf{H}_u + \mathbf{H}_w^T I_{11} \mathbf{H}_w - \mathbf{H}_u^T I_{12} \mathbf{H}_{w,x} + \mathbf{H}_{w,x}^T I_{22} \mathbf{H}_{w,x} \right) dx \tag{27}$$

The finite element equation for undamped dynamic analysis of the beam has the form

$$\mathbf{M}\ddot{\mathbf{D}} + \mathbf{K}\mathbf{D} = \mathbf{R}_{\mathrm{ex}} \tag{28}$$

where **D, M** and **K** are the total nodal displacement vector, mass and stiffness matrices, respectively; Fex is the total nodal load vector with the following form

$$\mathbf{R}_{\mathrm{ex}} = \left\{ 0 \ldots 0 \ldots 0 \underbrace{F_0 \cos(\Omega t)\mathbf{H}_w|_{x_e}}_{\text{element under loading}} 0 \ldots 0 \ldots 0 \right\}^T \tag{29}$$

The above nodal load vector contains all zero coefficients, except for the element currently under loading. The notation $\mathbf{H}_w|_{x_e}$ in Eq. (29) means that the shape function matrix $\mathbf{H}_w$ are calculated at x_e, which is the position of load F measured from the most left node of the element. The average acceleration method described in [16] is adopted herein to solve Eq. (28). By setting the right-hand side of

Eq.(28) to zeros, the equation becomes a free vibration problem, which can be solved by the standard value solver.

Results and Discussion

A computer code based on the developed formulation and described numerical algorithm is developed and employed to study the dynamic behavior of the beam in this Section. To this end, anFGM beam formed fromAl_2O_3 and SUS304 with the materials data given in Table 1 under a moving harmonic load $F=F_0\cos(\Omega t)$ with F_0=100 kN is considered here with. An aspect ratio L/h=20 is assumed, and a uniform increment time step, $\Delta t=\Sigma T/500$, where $\Sigma T=L/v$ is the total time for the load F to cross the beam, are employed for computation reported below.

Validation of derived formulation is firstly confirmed by comparing the numerical result of the present paper with the data available in the literature. In Table 2, the frequency parameters, $\overline{\omega} = \omega L^2 / h\sqrt{\rho_s / E_s}$ (with ω is the fundamental frequency and E_s, ρ_s are Young's modulus and mass density of steel), at various values of the UTR and NLTR of this paperare compared to the result obtained by the differential transform method in Ref. [6]. As observable from the table, the results of this paperare in good agreement with that of Ref [6]. To verify the formulation in evaluating the dynamic response of an FGM beam, the maximum dynamic amplification factor, max(DAF), and the corresponding velocity of a beam made of Al_2O_3 and Aluminum (Al), previously investigated in Ref. [8] are computed and the result is given in Table 3. Noting that the beam with data given in Ref. [8] were used in the analysis, and the DAF is defined in the same way as that of an isotropic beam carrying a moving load, that is

$$\mathrm{DAF} = \max\left[w_0(L/2,t)/w_{0\mathrm{st}}\right] \quad (30)$$

where is the maximum static deflection of the pure metal beam under a load F_0. As seen from Table 3, the maximum DAF and the corresponding velocity of present work are in good agreement with that of Ref. [8]. It is worth to mention that the results in Table 2 and Table 3 are converged by using twenty elements, and this number of elements will be utilized for the all the numerical examples.

The effect of material distribution on the dynamic behavior of FGM beam in the thermal environment can be seen from Figure 2, where the time histories for the normalized deflection are illustrated for various values of the grading index n and v=20 m/s, Ω=15 rad/s, ΔT=50K. In the figure and hereafter, the traveling time and the mid-span deflection are normalized by the total time and the maximum static deflection, that is $t^*=t/\Sigma T$ and $w^*=w_0(L/2,t)/w_{0st}$. As seen from Figure 2, at the given values of the moving load velocity, excitation frequency and temperature rise, the maximum mid-span deflection increases with the increase of the index n, regardless of the temperature type. The curves for the time histories obtained in the UTR are similar to that obtained in the NLTR, except for the higher amplitude.The increase of the mid-span deflection by raising the grading index n can also be seen from Figure 3 where the relation between the DAF and the index nis depicted for different temperature rises. The DAF steadily increase with the increase in the index n, irrespective of the temperature distribution. The DAF of the beam subjected to NLTR is smaller than that of the beam under UTR, but the relations between DAF and n of the two temperature distributions are very similar.

The influence of the temperature rise on the dynamic behavior of the FGM beam is illustrated in Figsure 4–6. The maximum mid-span deflection of the beam, as seen from Figure 4 increases by both the UTR and NLTR. The situation for the DAF, as can be observable from Figure 5, is similar, and the DAF increases with increasing the temperature rise. The influence of the UTR is more significant than that of the NLTR, and the DAF increases more significantly by the UTR. The curves exhibit the relation between the DAF and the moving load velocity have similar forms as that of a homogeneous beam subjected to a moving force [17], and the DAF experiences a repeated increase and decrease period before reaching a peak value, regardless of the temperature rise. The increase of the DAF by the temperature rise can also be seen from Table 4, where the DAF is given for various values of the moving load velocity, the temperature rise and the grading index n. Irrespective of the moving load velocity and the index n, the DAF in the table clearly increases by the temperature rise. The axial stress at the mid-span section, as seen from Fig. 6, also increases by the temperature rise, and the increase of the stress by UTR is more significant than by the NLTR. The stress in Figire 6 was calculated at the time when the load arrives at the mid-span and it was normalized by F_0/A.

In Figure 7, the time histories for the normalized mid-span deflection are depicted for various values of the excitation frequency Ω and n=3, v=20 m/s, ΔT=50K. The effect of the excitation frequency on the dynamic behavior of the beam is clearly seen from the figure. The number of vibrations which the beam executesincrease with

		n=0.1		n=0.2		n=0.5		n=1	
ΔT		Ref. [6]	Present work	Ref. [6]	Present work	Ref. [6]	Present work	Ref. [6]	Present work
20K	UTR	4.6536	4.6053	4.3867	4.3514	3.8974	3.8767	3.5193	3.5046
	LTR	4.7018	4.6598	4.4334	4.4089	3.9354	3.9384	3.5474	3.5678
40K	UTR	4.4516	4.3944	4.1782	4.1350	3.6779	3.6510	3.2925	3.2726
	LTR	4.6020	4.5603	4.3279	4.3093	3.8141	3.8380	3.4114	3.4659
80K	UTR	4.0148	3.9377	3.7212	3.6610	3.1834	3.1441	2.7693	2.7399
	LTR	4.3956	4.3546	4.1087	4.1031	3.5591	3.6292	3.1216	3.2531

Table 2: Comparison of frequency parameter of FGM porous beam in thermal environment.

	Present work	Ref. [8]		
n	max(DAF)	v (m/s)	max(DAF)	v (m/s)
0.2	1.0361	222	1.0344	222
0.5	1.1447	198	1.1444	198
1	1.2503	179	1.2503	179
2	1.3377	164	1.3376	164
Al_20_3	0.9329	252	0.9328	252
SUS_30_4	1.7326	132	1.7324	132

Table 3: Comparison of maximum amplification factor and corresponding velocity of FGM beam in room temperature.

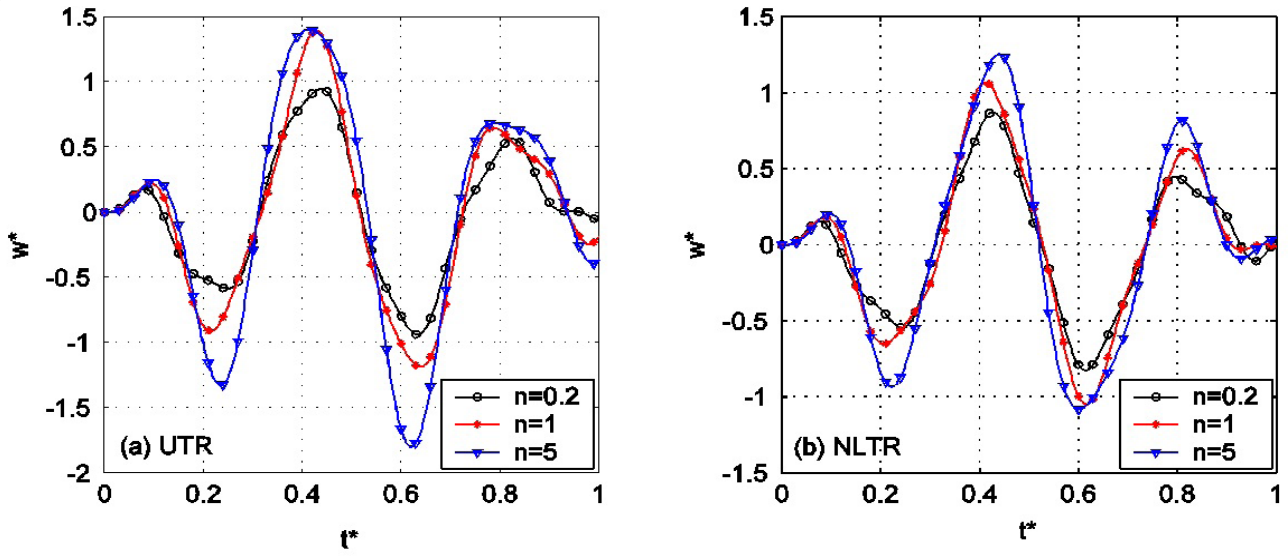

Figure 2: Time histories for normalized mid-span deflection for various values of index n(v=20 m/s, Ω=15 rad/s, ΔT=50K).

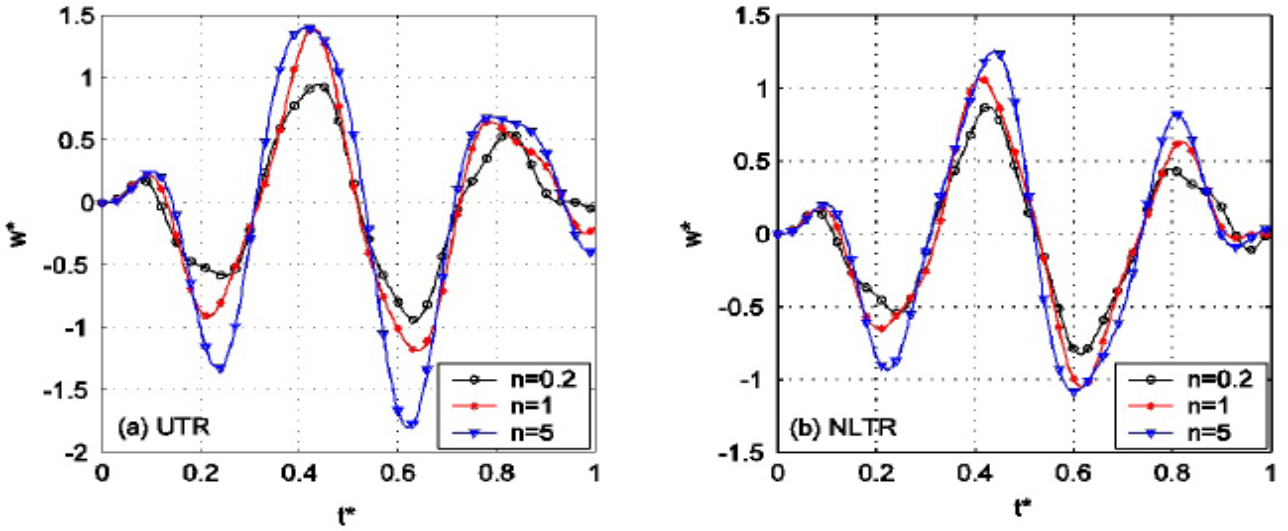

Figure 3: Relation between DAF and grading index nwithdifferent temperature rises (v=30 m/s, Ω=0).

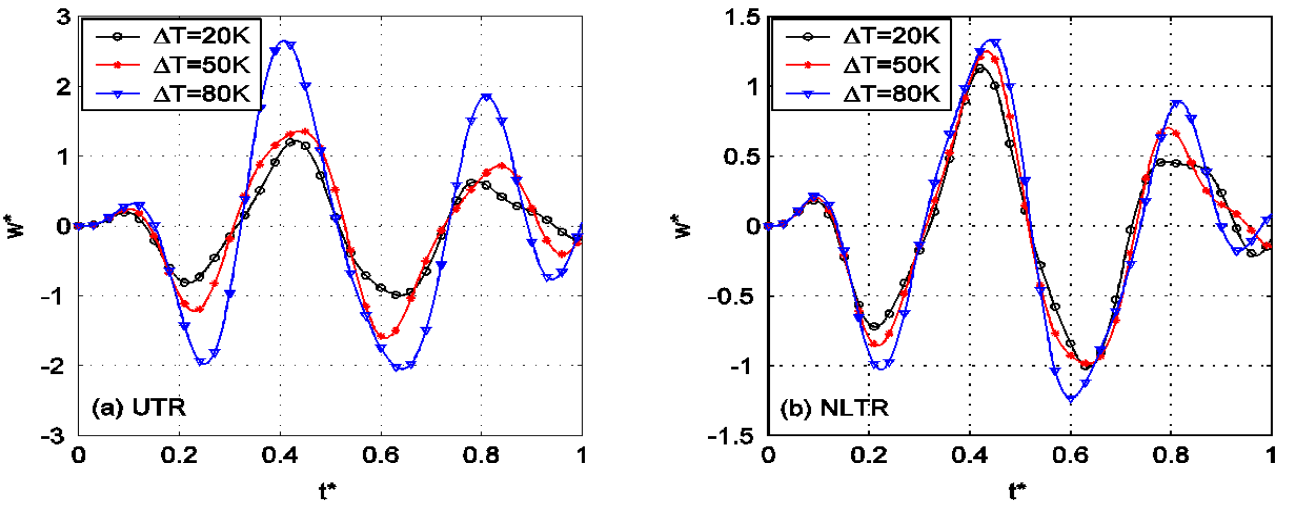

Figure 4: Effect of temperature rise on time histories for normalized mid-span deflection for n=3, v=20 m/s, Ω=15 rad/s.

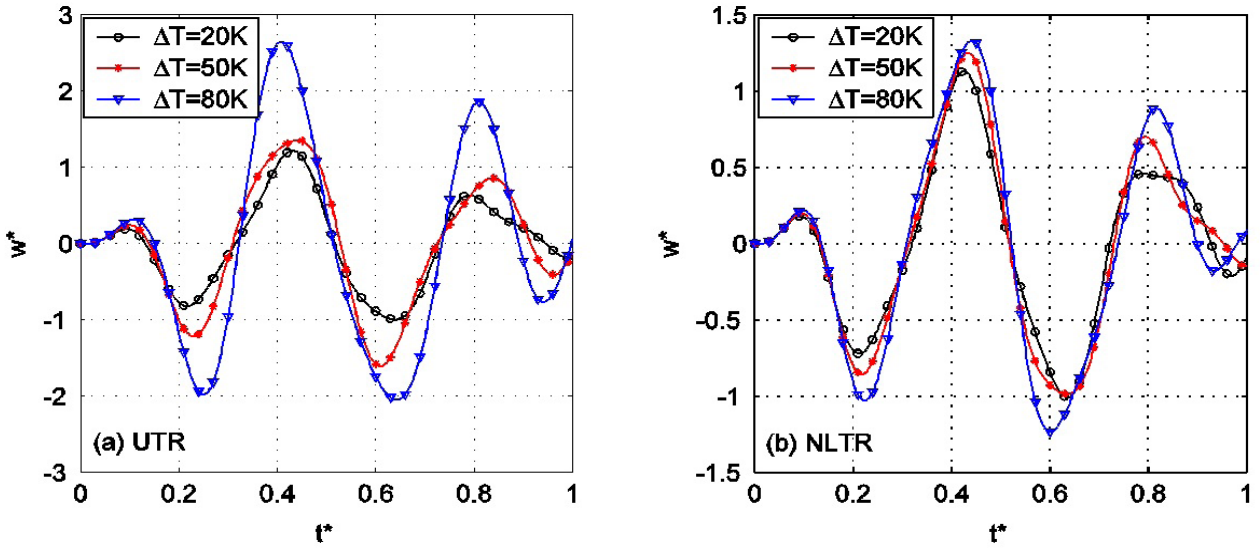

Figure 4: Effect of temperature rise on time histories for normalized mid-span deflection for n=3, v=20 m/s, Ω=15 rad/s.

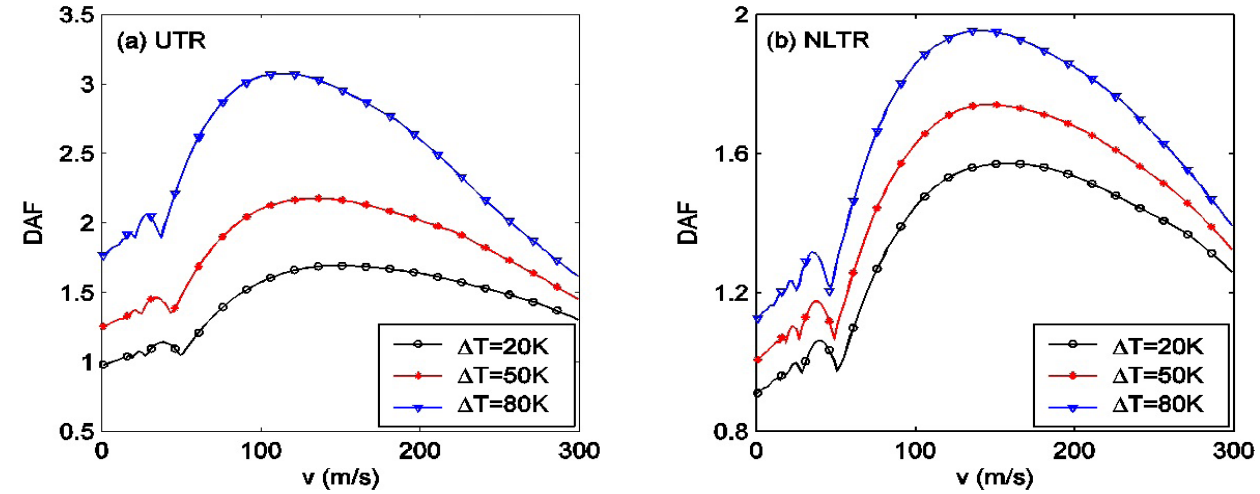

Figure 5: Relation between DAF and moving load velocity v for various temperature rises and n=3, Ω=0.

Temperature	v (m/s)	ΔT(K)	n=0.1	n=0.2	n=0.5	n=1	n=2	n=5
UTR	25	50	0.9173	0.9562	1.1114	1.2334	1.3043	1.4525
		100	1.2536	1.3929	1.6645	2.1392	2.6394	3.1685
	50	50	1.0034	1.0633	1.1657	1.2114	1.3902	1.6104
		100	1.3454	1.4349	1.7777	2.4255	3.1721	4.1644
NLTR	25	50	0.814	0.8442	0.9223	1.0174	1.083	1.1336
		100	0.9097	0.9404	1.0823	1.1994	1.2767	1.4233
	50	50	0.8761	0.9222	1.0056	1.0551	1.0671	1.1749
		100	0.9937	1.0473	1.1415	1.1883	1.3397	1.5744

Table 4: DAF for different values of moving load velocity, temperature rise and index n.

In Figure 7, the time histories for the normalized mid-span deflection are depicted for various values of the excitation frequency Ω and n=3, v=20 m/s, ΔT=50K.The effect of the excitation frequency on the dynamic behavior of the beam is clearly seen from the figure. The number of vibrations which the beam executesincrease with increasing the excitation frequency. The vibration amplitude is much higher for the excitation frequency near the fundamental frequency, which equals to 34.4359 rad/s and 38.4791 rad/s for the UTR and NLTR of the figure, respectively. The influence of the excitation frequency on the dynamic behavior of the beam can be seen more clearly from Fig. 8, where the relation between DAF and the excitation frequency is illustrated for different temperature rises and n=3, v=20 m/s.

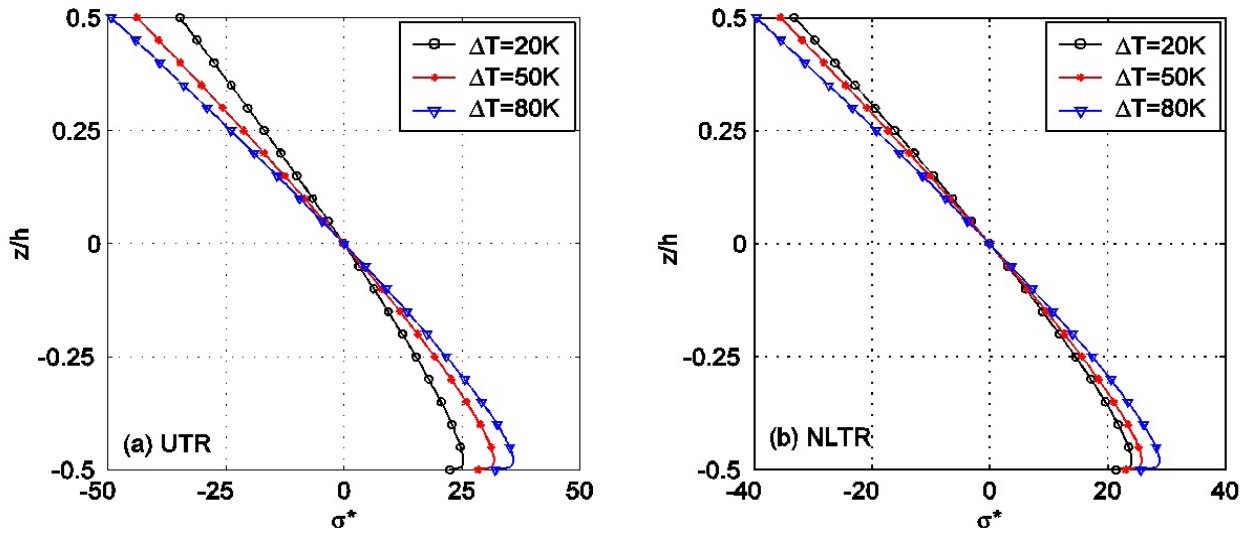

Figure 6: Effect of temperature rise on thickness distribution of normalized axial stress for n=0.3, v=20 m/s, Ω=0.

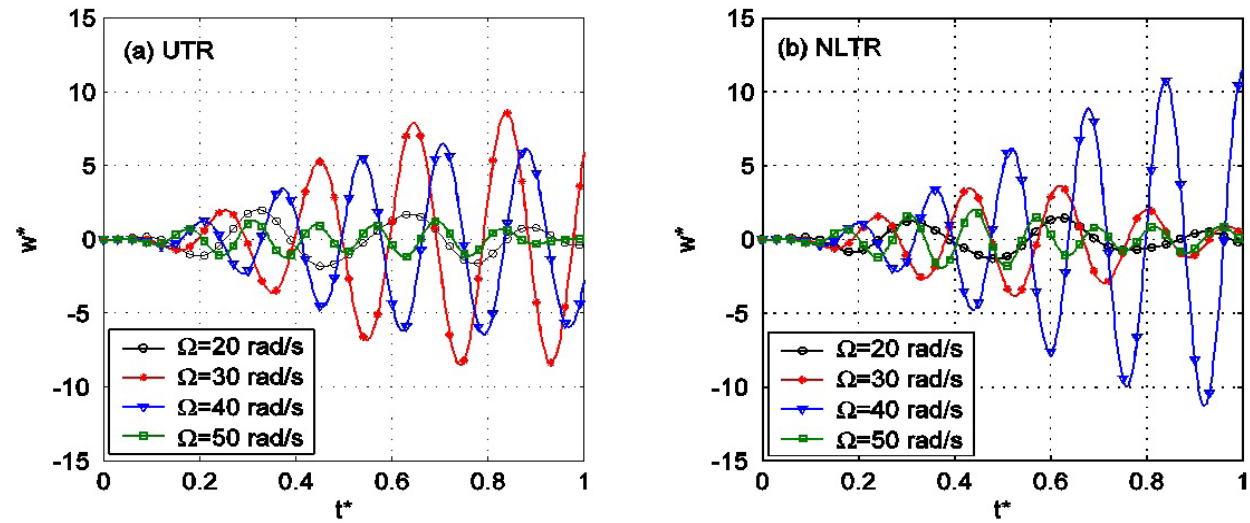

Figure 7: Time histories for normalized mid-span deflection for various values of excitation frequency n=3, v=20 m/s, ΔT=50K.

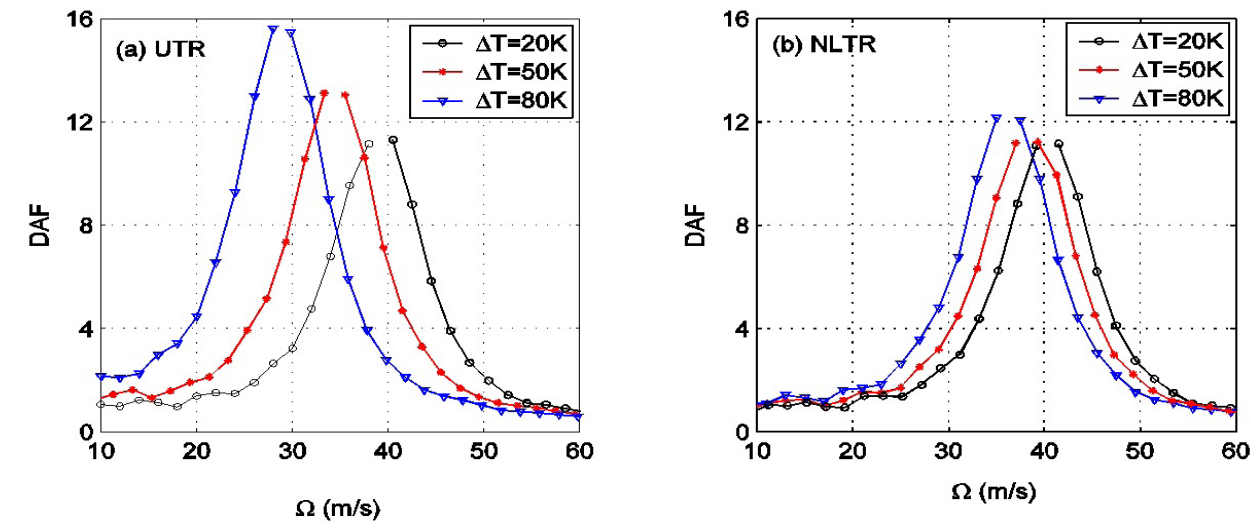

Figure 8: Relation between DAF and excitation frequency for different temperature rises and n=3, v=20 m/s.

The DAF rapidly increases when the excitation frequency approaches the fundamental frequency, irrespective of the temperature rise. Since the damping effect is ignored in the present work, the resonance will occur, and the DAF becomes infinity when the excitation frequency equals to the fundamental frequency. The excitation frequency at which the resonance can occur, as seen from Figure 8, changes with the temperature of the environment, and this should be taken into consideration in designing FGM beams subjected to moving harmonic loads. The resonant frequencies corresponding to the curves in Fig. 8 are 39.0262 rad/s, 34.4359 rad/s, 28.9872 rad/s for the UTR and 40.4788 rad/s, 38.4791 rad/s and 36.3454 rad/s for the NLTR.

Conclusion

The dynamic behavior of FGM beams in the thermal environment due to a moving harmonic load was investigated. The material properties are assumed to be temperature-dependentand they are graded in the thickness direction by the power-law distribution. Equations of motion derived from Hamilton's principle and they are solved by a finite element formulation in combination with the Newmark method. The validation of the derived formulation has been confirmed by comparing the obtained numerical result with the data available in the literature. A parametric study was carried out on a beam with simply supported ends to highlight the influence of the material distribution, the temperature rise, the moving load velocity and excitation frequency on the dynamic behavior of the beam. The main conclusions of the paper can be summarized as follows.

- The dynamic characteristics of FGM beams under a moving load, including the mid-span dynamic deflection, DAF and axial stress are significantly influenced by the temperature, and they are increasedby the increase of the temperature rise. Among the two types of temperature distribution considered in the present work, the UTR has a stronger effect on the dynamic response than the NLTR does.

- The excitation frequency plays an important role in the dynamic behavior of the FGM beams due to moving harmonic load, and the resonance can occur when the excitation frequency and the fundamental frequency are identical. The resonant frequency, however changes with the change of the environment temperature, and this should be taken into account in designing the FGM beams in a thermal environment subjected to moving harmonic loads.

Competing Interestes

The authors declare that they have no competing interestes.

References

1. Koizumi M (1997) FGM activities in Japan. Compos Pt B Eng 28: 1-4.
2. Kim YW (2005) Temperature dependent vibration analysis of functionally graded rectangular plates. J Sound Vib 284: 531-549.
3. Pradhan SC, Murmu T (2009) Thermo-mechanical vibration of FGM sandwich beam under variable elastic foundations using differential quadrature method. J Sound Vib 321: 342-362.
4. Mahi A, Adda Bedia EA, Tounsi A, Mechab I (2010) An analytical method for temperature-dependent free vibration analysis of functionally graded beams with general boundary conditions. Compos Struct 92: 1877-1887.
5. Wattanasakulpong N, Gangadhara Prusty B, Kelly DW (2011) Thermal buckling and elastic vibration of third-order shear deformable functionally graded beams. Int J Mech Sci 53: 734-743.
6. Ebrahimi F, Ghasemi F, Salari E (2015) Investigating thermal effects on vibration behavior of temperature-dependent compositionally graded Euler beams with porosities. Meccanica 51: 223.
7. Frýba L (1999) Vibration of solids and structures under moving loads. (Third edition), Thomas Telford House, Prague.
8. Şimşek M, Kocatürk T (2009) Free and forced vibration of a functionally graded beam subjected to a concentrated moving harmonic load. Compos Struct 90: 465-473.
9. Şimşek M (2010a) Vibration analysis of a functionally graded beam under a moving mass by using different beam theories. Compos Struct 92: 904-917.
10. Şimşek M (2010b) Non-linear vibration analysis of a functionally graded Timoshenko beam under action of a moving harmonic load. Compos Struct 92: 2532-2546.
11. Khalili SMR, Jafari AA, Eftekhari SA (2010) A mixed Ritz-DQ method for forced vibration of functionally graded beams carrying moving loads. Compos Struct 92: 2497-2511.
12. Rajabi K, Kargarnovin MH, Gharini M (2013) Dynamic analysis of a functionally graded simply supported Euler-Bernoulli beam to a moving oscillator, Acta Mech 224: 425-446.
13. Nguyen DK, Gan BS, Le TH (2013) Dynamic response of non-uniform functionally graded beams subjected to a variable speed moving load, J Comput Sci Tech(JSME) 7: 12-27.
14. Gan BS, Trinh TH, Le TH, Nguyen DK (2015) Dynamic response of non-uniform Timoshenko beams made of axially FGM subjected to multiple moving point loads. Struct Eng Mech 53: 981-995.
15. Touloukian YS (1967) Thermophysical properties of high temperature solid materials. Macmillan, New York.
16. Géradin M, Rixen D (1997) Mechanical vibrations: Theory and application to structural dynamics. 2nd edition John Wiley & Sons, Chichester.
17. Olsson M (1991) On the fundamental moving load problem. J Sound Vib 152: 229-307.